Multifidelity Statistical Analysis of Large Eddy Simulations in Scramjet Computations

Xun Huan*, Gianluca Geraci†, Cosmin Safta‡, Michael S. Eldred§,
Khachik Sargsyan¶, Zachary P. Vane*, Joseph C. Oefelein‖, Habib N. Najm**
Sandia National Laboratories, 7011 East Avenue, Livermore, CA 94550

The development of scramjet engines is an important research area for advancing hypersonic and orbital flights. Progress towards optimal engine designs requires accurate and computationally affordable flow simulations, as well as uncertainty quantification (UQ). While traditional UQ techniques can become prohibitive under expensive simulations and high-dimensional parameter spaces, polynomial chaos (PC) surrogate modeling is a useful tool for alleviating some of the computational burden. However, non-intrusive quadrature-based constructions of PC expansions relying on a single high-fidelity model can still be quite expensive. We thus introduce a two-stage numerical procedure for constructing PC surrogates while making use of multiple models of different fidelity. The first stage involves an initial dimension reduction through global sensitivity analysis using compressive sensing. The second stage utilizes adaptive sparse quadrature on a multifidelity expansion to compute PC surrogate coefficients in the reduced parameter space where quadrature methods can be more effective. The overall method is used to produce accurate surrogates and to propagate uncertainty induced by uncertain boundary conditions and turbulence model parameters, for performance quantities of interest from large eddy simulations of supersonic reactive flows inside a scramjet engine.

I. Introduction

The development of supersonic combusting ramjet (scramjet) engines is an important research area for advancing hypersonic and orbital flights. Progress towards optimal engine designs requires accurate and computationally affordable flow simulations, as well as uncertainty quantification (UQ). Characterizing and predicting combustion properties under extreme flow conditions that are also coupled with the multiscale and multiphysics processes presents a highly challenging and expensive undertaking for even a single simulation. Traditional UQ techniques, typically involving direct explorations of the parameter space through repeated simulations, would be prohibitive. Indeed, only a few UQ studies existed for scramjet computations,[1,2] while recent developments in both algorithms and computational power have enabled new investigations involving large eddy simulation (LES) datasets in this application.[3–6]

We concentrate on a scramjet configuration studied under the HIFiRE (Hypersonic International Flight Research and Experimentation) program,[7,8] which has been the target of a mature experimental campaign with accessible data through its HIFiRE Flight 2 (HF2) project.[9,10] The HF2 payload, depicted in Fig. 1(a), involves a cavity-based hydrocarbon-fueled dual-mode scramjet that enables transition from ramjet mode (subsonic flow in the combustor) to scramjet mode (supersonic flow in the combustor) through a

*Postdoctoral Appointee, Combustion Research Facility, MS9051, AIAA Member.
†Postdoctoral Appointee, Optimization and Uncertainty Estimation, Sandia National Laboratories, 1515 Eubank SE, MS1318, Albuquerque, NM 87123, AIAA Member.
‡Principal Member of Technical Staff, Quantitative Modeling and Analysis, MS9159, AIAA Senior Member.
§Distinguished Member of Technical Staff, Optimization and Uncertainty Estimation, Sandia National Laboratories, 1515 Eubank SE, MS1318, Albuquerque, NM 87123, AIAA Associate Fellow.
¶Principal Member of Technical Staff, Combustion Research Facility, MS9051.
‖Distinguished Member of Technical Staff, Combustion Research Facility, MS9051, AIAA Associate Fellow.
**Distinguished Member of Technical Staff, Combustion Research Facility, MS9051, AIAA Member.

variable Mach number flight trajectory. The isolator/combustor was derived from a series of legacy configurations,[10,11] while the forebody, inlet, and nozzle were designed subsequently.[12,13] A ground test rig, designated the HIFiRE Direct Connect Rig (HDCR) (Fig. 1(b)), was developed to duplicate the isolator/combustor layout of the flight test hardware, and to provide ground-based data for comparisons with flight data, verifying engine performance and operability, and designing fuel delivery schedule.[14,15] Mirroring the HDCR setup, we aim to simulate and assess flow characteristics inside the isolator/combustor portion of the scramjet.

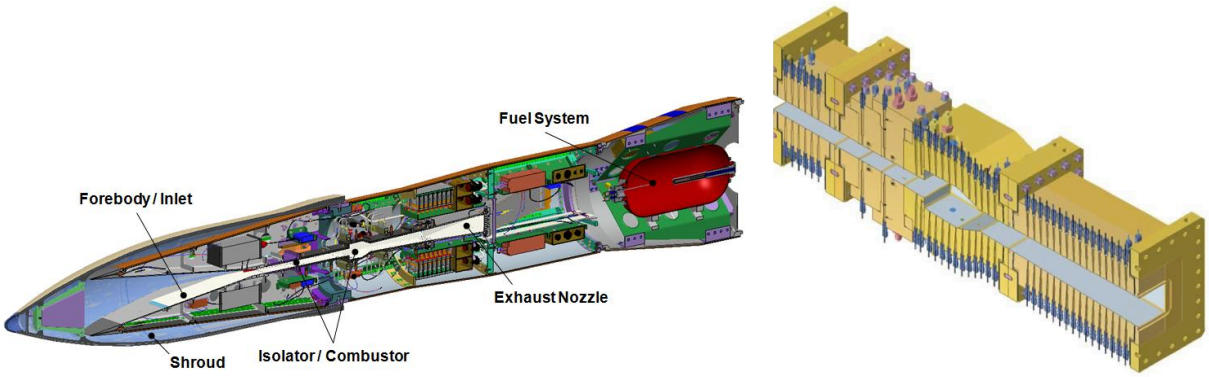

(a) HIFiRE Flight 2 payload (b) HDCR

Figure 1. HIFiRE Flight 2 payload and HDCR cut views.

One important aspect of UQ analysis is surrogate modeling. A surrogate model is often computationally much less expensive compared to the full physical model while achieving a desirable level of accuracy. It is valuable in relieving computational burden of multi-query procedures and allowing efficient evaluations of statistical properties for quantities of interest (QoIs). One useful surrogate choice is the polynomial chaos (PC) expansion. A PC expansion[16–19] is a spectral representation of a random variable (quantity), and provides a convenient means for propagating uncertainty that does not require direct Monte Carlo simulations of the expensive full model. The goal of this paper is to present a numerical procedure for constructing PC surrogates in a multifidelity (MF) setting—i.e., when multiple models of different fidelity are available. Intuitively, MF approaches[20–23] can allow the extraction of information from inexpensive lower-fidelity simulations when possible, and resort to expensive higher-fidelity models only when needed, thus achieving an overall resource-efficient computation. At the same time, when model output QoIs are expected to change smoothly with respect to input variations, quadrature-based techniques may be adopted to construct the PC surrogates using a smaller number of samples for a given accuracy target compared to standard regression techniques. However, even with sparsifying and adaptive enhancements,[24–26] quadrature computation can become impractical for high dimensions. We thus introduce the following two-stage workflow:

1. perform an initial dimension reduction through global sensitivity analysis (GSA)[27,28] using compressive sensing (CS)[29,30] based on randomized samples, and

2. employ adaptive sparse quadrature (ASQ) to compute PC surrogate coefficients for a MF expansion in the reduced parameter space.

The overall method is demonstrated on LES of supersonic reactive flows inside the HIFiRE scramjet combustor chamber.

The paper is structured as follows. Section II describes the physics and solver used for simulating the reactive flows. We then introduce the aforementioned two-stage numerical procedure for constructing PC surrogates in Sec. III. Results and discussions on the scramjet application are presented in Sec. IV. The paper ends with conclusions in Sec. V.

II. Reactive Flow Simulations for the HDCR

We simulate reactive flows inside the HDCR combustor. A schematic of this configuration is shown in Fig. 2. The rig consists of a constant-area isolator (planar duct) attached to a combustion chamber. It

includes four primary injectors that are mounted upstream of flame stabilization cavities on both the top and bottom walls. Four secondary injectors along both walls are positioned downstream of the cavities. The primary fuel injectors are located at 244 mm downstream from the inlet and aligned at 15° from the wall, while the secondary injectors are at 419 mm and aligned at 90° from the wall. All injectors have a diameter of $d = 3.175$ mm. Flow travels from left to right in the x-direction (streamwise), and the geometry is symmetric about the centerline in the y-direction. Numerical simulations take advantage of this symmetry by considering a domain that covers only the bottom half of this configuration. To further reduce the computational cost, we consider one set of primary/secondary injectors and impose periodic conditions in the z-direction (spanwise). The overall computational domain is highlighted by the red lines in Fig. 2.

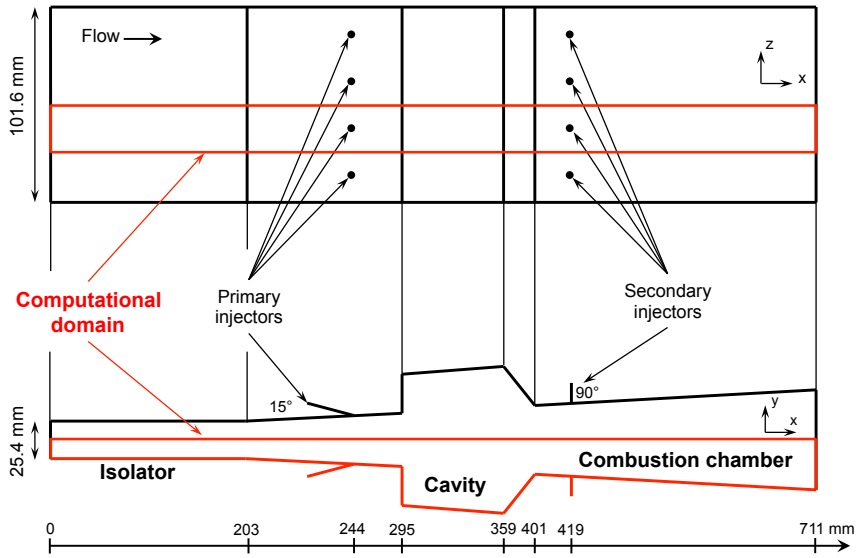

Figure 2. Schematic of the full computational domain.

JP-7 surrogate fuel[31] is inserted through the injectors, containing 36% methane and 64% ethylene by volume. A reduced, three-step mechanism[32,33] is employed to characterize the combustion process:

$$\mathrm{CH_4} + 2(\mathrm{O_2} + f_{\mathrm{NO}}\mathrm{N_2}) \rightarrow \mathrm{CO_2} + 2\mathrm{H_2O} + 2f_{\mathrm{NO}}\mathrm{N_2} \tag{1}$$

$$\mathrm{C_2H_4} + 3(\mathrm{O_2} + f_{\mathrm{NO}}\mathrm{N_2}) \rightarrow 2\mathrm{CO_2} + 2\mathrm{H_2O} + 3f_{\mathrm{NO}}\mathrm{N_2} \tag{2}$$

$$2\mathrm{CO} + \mathrm{O_2} \rightarrow 2\mathrm{CO_2}, \tag{3}$$

where $f_{\mathrm{NO}} = 0.79/0.21$ is the ratio between the mole fractions of $\mathrm{N_2}$ and $\mathrm{O_2}$ in the oxidizer streams. Arrhenius formulations of the kinetic reaction rates are adopted, and the parameters are tuned under a separate study to match the heat release rate to a reference mechanism using GRIMech 3.0[34] over a range of equivalence ratios[35] and also to retain robust/stable combustion in the current simulations.

LES calculations are performed using the RAPTOR code framework.[36,37] The theoretical framework solves the fully coupled conservation equations of mass, momentum, total-energy, and species for a chemically reacting flow. It is designed to handle high Reynolds number, high-pressure, real-gas and/or liquid conditions over a wide Mach operating range. It also accounts for detailed thermodynamics and transport processes at the molecular level. RAPTOR is designed specifically for LES using non-dissipative, discretely conservative, staggered, finite-volume differencing, which eliminates numerical contamination of the subfilter models due to artificial dissipation and provides discrete conservation that is imperative for high quality LES. Representative results and case studies using RAPTOR can be found in investigations by Oefelein *et al.*[38–40]

In our numerical study, we allow a total of 11 input parameters to be variable and uncertain. These parameters, shown in Table 1 along with their uncertainty distributions, reflect sources of uncertainty in the inlet and fuel inflow boundary conditions as well as turbulent model parameters. The distributions are assumed uniform across the ranges stated in the table. We focus on two QoIs that are useful indicators of the overall scramjet performance: (1) burned equivalence ratio (ϕ_B) and (2) stagnation pressure loss ratio ($R_{\bar{P}}$). All QoIs are also time-averaged quantities.

- **Burned equivalence ratio (ϕ_B)** is defined as $\phi_B \equiv \phi_T \eta_c$, where ϕ_T is the total equivalence ratio imposed on the system, and η_c is the combustion efficiency based on static enthalpy quantities:[11,15]

$$\eta_c = \frac{H(T_{\text{ref}}, Y_{\text{e}}) - H(T_{\text{ref}}, Y_{\text{ref}})}{H(T_{\text{ref}}, Y_{\text{e,ideal}}) - H(T_{\text{ref}}, Y_{\text{ref}})}. \tag{4}$$

  Here H is the total static enthalpy, the "ref" subscript indicates a reference condition derived from the inputs, the "e" subscript is for the exit, and the "ideal" subscript is for the ideal condition where all fuel is burned to completion. The reference condition corresponds to that of a hypothetical non-reacting mixture of all inlet air and fuel at thermal equilibrium. The numerator, $H(T_{\text{ref}}, Y_{\text{e}}) - H(T_{\text{ref}}, Y_{\text{ref}})$, thus reflects the global heat released during the combustion, while the denominator represents the total heat release available in the fuel-air mixture.

- **Stagnation pressure loss ratio ($R_{\bar{P}}$)** is defined as

$$R_{\bar{P}} = 1 - \frac{P_{s,e}}{P_{s,i}}, \tag{5}$$

  where $P_{s,e}$ and $P_{s,i}$ are the wall-normal-averaged stagnation pressure quantities at the exit and inlet planes, respectively.

III. Multifidelity Polynomial Chaos Surrogates

In this section, we introduce a two-stage numerical procedure for constructing PC surrogates in a MF setting. We first present some background before describing the two steps in detail. Consider a set of M models indexed by $m = 1, \ldots, M$, where, for simplicity, $m = 1$ represents the lowest fidelity and $m = M$ the highest. Furthermore, we assume these models share common input parameters λ and output QoI $f_m(\lambda)$. The objective is to construct a PC surrogate for QoI from the highest-fidelity model, $f_M(\lambda)$.

Conventional single-model approaches invoke PC construction using only the highest-fidelity model $f_M(\lambda)$. When lower-fidelity, computationally less expensive counterparts are available, their inclusion can potentially improve the overall construction efficiency. We seek to achieve such a MF form through the following telescopic expansion on $f_M(\lambda)$:

$$f_M(\lambda) = \sum_{m=1}^{M} f_{\Delta m}(\lambda), \tag{6}$$

where $f_{\Delta m}(\lambda) \equiv f_m(\lambda) - f_{m-1}(\lambda)$, and $f_0(\lambda) \equiv 0$. A separate PC can then be produced to approximate each term, and summed together to arrive at an overall PC for $f_M(\lambda)$:

$$f_M(\lambda) \approx \tilde{f}_M(\lambda(\xi)) = \sum_{m=1}^{M} \tilde{f}_{\Delta m}(\lambda(\xi)), \tag{7}$$

where $\tilde{f}$ are PC surrogates that are direct functions of basic random vector ξ (to be described shortly). More specifically, the PC for a QoI-difference in Eqn. (6) has the form

$$f_{\Delta m}(\lambda) \approx \tilde{f}_{\Delta m}(\lambda(\xi)) = \sum_{\beta \in \mathcal{J}} c_\beta \Psi_\beta(\xi_1, \xi_2, \ldots, \xi_{n_s}), \tag{8}$$

where $\beta = (\beta_1, \beta_2, \ldots, \beta_{n_s}), \forall \beta_j \in \mathbb{N}_0$ is a multi-index, n_s is the system stochastic dimension, $\mathcal{J}$ is an index set for β (e.g., *total-order* expansion of degree p involves $\mathcal{J} = \{\beta : |\beta| \leq p\}$), ξ_j are independent and identically distributed (i.i.d.) basic random variables often possessing a standard form (e.g., uniform or standard Gaussian), c_β are the expansion coefficients, and Ψ_β are the multivariate orthonormal polynomials written as products of univariate orthonormal polynomials

$$\Psi_\beta(\xi_1, \xi_2, \ldots, \xi_{n_s}) = \prod_{j=1}^{n_s} \psi_{\beta_j}(\xi_j). \tag{9}$$

ψ_{β_j} is then a polynomial of degree β_j in the independent variable ξ_j, and orthonormal with respect to the density of ξ_j (i.e., $p(\xi_j)$):

$$\mathbb{E}\left[\psi_k(\xi_j)\psi_n(\xi_j)\right] = \int_{\Xi} \psi_k(\xi_j)\,\psi_n(\xi_j)\,p(\xi_j)\,d\xi_j = \delta_{k,n}, \tag{10}$$

with Ξ being the support of $p(\xi_j)$. Different choices of ξ_j and ψ_m are available under the generalized Askey family.[41] The input parameters encountered in our application are endowed with uniform distributions, we thus employ uniform $\xi_j \sim \mathcal{U}(-1,1)$ and Legendre polynomials which then allow exact PC to be formed for inputs λ using linear expansions.

Since our scramjet LES model is highly complex and only available as a black-box in practice, and also for accommodating flexible choices of QoIs, we elect to take a non-intrusive approach to compute the expansion coefficients. Furthermore, we expect the QoIs to behave smoothly, and hence quadrature methods would be ideal to take advantage of this regularity. As quadrature computations are most effective and affordable in smaller dimensions, we perform an initial dimension reduction step using GSA to facilitate such an environment.

III.A. Initial dimension reduction through global sensitivity analysis

We utilize GSA to identify the most important uncertain input parameters that induce the statistical properties of QoIs. In contrast to local sensitivity analysis, GSA reflects the overall sensitivity characteristics across the *entire* uncertain input domain. Specifically, we adopt a *variance-based* assessment: loosely speaking, the variance of a QoI can be decomposed into contributions from the variance of each input. With λ denoting the vector of all input parameters, Sobol sensitivity indices[42] can be computed to rank the components λ_i in terms of their variance contributions to that of a QoI $f(\lambda)$. Furthermore, we focus on the *total effect sensitivity* index, which measures variance contributions from *all* terms (including products) that involve the ith parameter:

$$S_{T_i} = \frac{\mathbb{E}_{\lambda_{\sim i}}\left[\mathrm{Var}_{\lambda_i}\left(f(\lambda)|\lambda_i\right)\right]}{\mathrm{Var}\left(f(\lambda)\right)}. \tag{11}$$

The notation $\lambda_{\sim i}$ refers to all components of λ *except* the ith component.

We compute S_{T_i} for all parameters in the full initial parameter space by constructing a crude PC expansion for the QoIs. We emphasize that the objective of this stage is to identify the relative importance between different inputs, and not to build a high accuracy surrogate model. Therefore, a low-order PC expansion using few evaluations would suffice. For example, this can be achieved by solving the regression problem for the following linear system $Ax = y$:

$$\underbrace{\begin{bmatrix} \Psi_{\beta^1}(\xi^{(1)}) & \cdots & \Psi_{\beta^q}(\xi^{(1)}) \\ \vdots & & \vdots \\ \Psi_{\beta^1}(\xi^{(n)}) & \cdots & \Psi_{\beta^q}(\xi^{(n)}) \end{bmatrix}}_{A} \underbrace{\begin{bmatrix} c_{\beta^1} \\ \vdots \\ c_{\beta^q} \end{bmatrix}}_{x} = \underbrace{\begin{bmatrix} f(\lambda(\xi^{(1)})) \\ \vdots \\ f(\lambda(\xi^{(n)})) \end{bmatrix}}_{y}, \tag{12}$$

where Ψ_{β^q} refers to the qth basis function, c_{β^n} is the coefficient corresponding to that basis, and $\xi^{(n)}$ is the nth regression point. When $n \geq p$, the system is overdetermined and ordinary least squares can be used; when $n < p$, the system is underdetermined and CS techniques[29,30] may be employed to facility recovery of sparse solutions. For example, one CS formulation is the unconstrained least absolute shrinkage and selection operator (LASSO):

$$\min_x \| Ax - y \|_2^2 + \mu \| x \|_1, \tag{13}$$

where μ is a regularization constant that balances between data-fitting and sparsity. While various efficient off-the-shelf LASSO solvers are available, the results in this paper are produced from the alternating direction method of multipliers (ADMM) solver.[43,44] A numerical investigation of several other solvers together with cross-validation tuning of μ and a stop-sampling rule for sequential data acquisition was previously performed for a non-reacting jet-in-crossflow setting under a simplified HDCR geometry.[45]

Once this initial PC $\tilde{f}$ becomes available, its corresponding S_{T_i} can be estimated directly from the expansion coefficients:

$$S_{T_i} = \frac{1}{\mathrm{Var}\left(\tilde{f}\right)} \sum_{\beta \in \mathcal{J}_{T_i}} c_\beta^2, \text{ where } \mathcal{J}_{T_i} = \{\beta \in \mathcal{J} : \beta_i > 0\}, \tag{14}$$

where the variance is

$$\mathrm{Var}\left(\tilde{f}\right) = \sum_{0 \neq \beta \in \mathcal{J}} c_\beta^2. \tag{15}$$

With S_{T_i} computed, the input parameters with the highest values can then be retained, leading to a lower dimensional parameter space where quadrature methods can be deployed to construct an accurate PC surrogate.

In the numerical study, we also compare two decision-making paths for the dimension reduction process. In the first, S_{T_i} values are computed for each of the M models separately. The resulting reduced space, for example, may be chosen to be the union of parameters from all models that reach some threshold. However, such an approach implicitly suggests all models are equally important, and it is unclear whether the inclusion of high-index parameters from lower-fidelity models would be appropriate or even necessary. We thus explore an alternative decision-making path that is more goal-oriented, that employs the MF form in Eqn. (7) and builds a single PC expansion targeting the highest-fidelity model. We assess the quality of the two paths empirically by observing S_{T_i} as the number of high-fidelity evaluations is varied.

III.B. Adaptive sparse quadrature for multifidelity expansion

Once the reduced parameter space is established, we seek to construct an accurate PC surrogate using ASQ under a MF setting. This is accomplished by computing expansion coefficients via orthogonal projections of QoI onto the subspace spanned by the basis functions, a procedure known as the non-intrusive spectral projection (NISP):

$$c_\beta = \mathbb{E}\left[f_{\Delta m}(\lambda)\Psi_\beta\right] \approx \int_\Xi \left[f_m\left(\lambda(\xi)\right) - f_{m-1}\left(\lambda(\xi)\right)\right] \Psi_\beta(\xi) p(\xi)\, d\xi. \tag{16}$$

In general, the integrals can only be estimated numerically and approximately, and quadrature methods can offer fast convergence by taking advantage of integrand regularity.

We employ a straightforward strategy for constructing $\tilde{f}_M(\lambda(\xi))$ in Eqn. (7) that involves performing quadrature integration on each term separately. Each integration is computed via the ASQ method introduced by Gerstner and Griebel,[26] which uses an adaptive refinement based on building Smolyak sparse quadrature[24,25] in different dimensions. Such an approach is convenient and does not require any modifications from the conventional ASQ method, but it may be inefficient since there is no prioritization between adaptation across the different integral terms. While not implemented in the current work, a next step involves a procedure[21] that performs adaptation globally across all terms and takes into account of both integral improvement as well as model costs.

Once we have PC surrogates for the QoIs in the reduced parameter space, we can perform uncertainty propagation and generate QoI samples to characterize its statistical properties. Furthermore, summary statistics can be extracted from the PC expansions; for example, the QoI mean is the constant term of the expansion, and the variance can be computed via Eqn. (15).

IV. Numerical Results

Two models ($M = 2$) are considered in this study: 2D simulations with grid resolutions where cell sizes are (1) $d/8$ and (2) $d/16$ ($d = 3.175$ mm is the injector diameter). A total of 11 uncertain input parameters are adopted and shown in Table 1 along with their uncertainty distributions—this is the full parameter space. The conditions for the primary injector are imposed to match an equivalence ratio of $\phi_p = 0.15$, while for the secondary injector $\phi_s = 0.5$, leading to a total equivalence ratio $\phi_T = \phi_p + \phi_s = 0.65$. We seek to characterize the statistical properties on two performance QoIs defined in Sec. II: burned equivalence ratio (ϕ_B) and stagnation pressure loss ratio ($R_{\bar{P}}$).

Parameter	Range	Description
Inlet boundary conditions:		
p_0	$[1.406, 1.554] \times 10^6$ Pa	Stagnation pressure
T_0	$[1472.5, 1627.5]$ K	Stagnation temperature
M_0	$[2.259, 2.761]$	Mach number
I_i	$[0, 0.05]$	Turbulence intensity horizontal component
R_i	$[0.8, 1.2]$	Ratio of turbulence intensity vertical to horizontal components
L_i	$[0, 8] \times 10^{-3}$ m	Turbulence length scale
Fuel inflow boundary conditions:		
I_f	$[0, 0.05]$	Turbulence intensity magnitude
L_f	$[0, 1] \times 10^{-3}$ m	Turbulence length scale
Turbulence model parameters:		
C_R	$[0.01, 0.06]$	Modified Smagorinsky constant
Pr_t	$[0.5, 1.7]$	Turbulent Prandtl number
Sc_t	$[0.5, 1.7]$	Turbulent Schmidt number

Table 1. Uncertain model input parameters. The uncertain distributions are assumed uniform across the ranges shown.

We begin by performing an initial dimension reduction through GSA by carrying out 256 simulations at randomly sampled input values for both $d/8$ and $d/16$ models. For each model, a total-order degree 3 (i.e., $\mathcal{J} = \{\beta : |\beta| \leq 3\}$) PC surrogate is constructed using the CS techniques described in Sec. III.A, and their corresponding Sobol indices are shown in Fig. 3. These results are also verified using PC surrogates of degrees 1 and 2 and with other CS solvers, all of which produced similar index values. One possible decision-making path to use this information for dimension reduction involves identifying the union of parameters from both models and QoIs that reach a given threshold. This is a compromising procedure where we take into account the GSA results from both models. Input parameters T_0 and M_0 overwhelmingly dominate in all cases; we also decide to include C_R and Sc_t, which possess the next highest indices in $d/8$ and $d/16$, respectively. The result is a four-dimensional input space. One may also choose to include Pr_t, which has the next highest index from $d/8$, but we exclude it in this study to keep the reduced dimensionality at four.

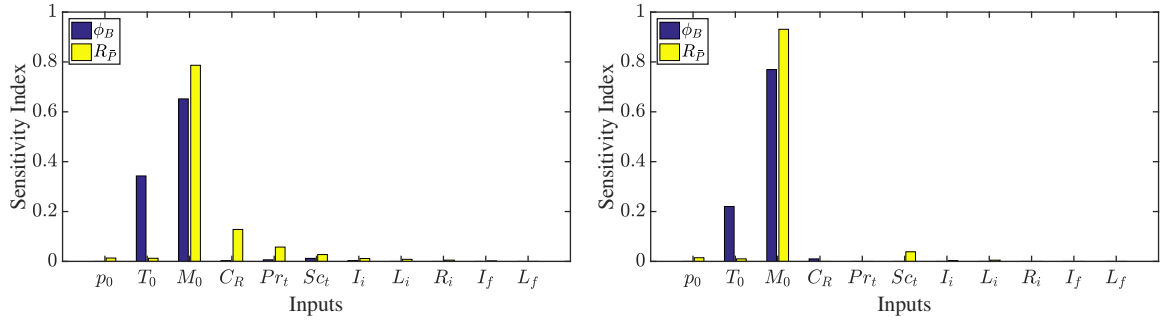

(a) $d/8$ model (b) $d/16$ model

Figure 3. Sobol indices (total effect sensitivity) for $d/8$ and $d/16$ models, QoIs ϕ_B and $R_{\bar{P}}$.

The above decision-making path implicitly suggests GSA results from all models are equally important. However, conflicting situations may exist. For example in Fig. 3, the high-fidelity model provides strong evidence suggesting C_R is not important for either QoI, whereas the low-fidelity model is not as conclusive. A conservative, but expensive solution is to keep all such parameters. Other factors to be considered also include the relative trustworthiness of the models and the quality of the GSA results. A rigorous and systematic combination of these elements is not straightforward, and an injection of subjectivity is

unavoidable. We thus explore an alternative decision-making path that directly targets the higher-fidelity model through the MF form.

Let the *direct* approach represent the aforementioned procedure that produced Fig. 3(b) (i.e., requires only $d/16$ simulations), and the *MF* approach represent GSA results based on the MF form in Eqn. (7). In the MF approach, we construct a PC surrogate for each term in the expansion separately, add together the PC surrogates, and then compute the Sobol indices. This approach may be useful if, for example, only a small number of $d/16$ runs are available and a direct computation would lead to high variance results. Assuming $d/16$ runs are the computationally dominating simulations and also to simplify comparisons, we always utilize the full set of 256 $d/8$ runs to construct the PC surrogate for the lower-fidelity term, while we compare the Sobol indices as the number of $d/16$ samples varies. The sensitivity indices for T_0, M_0, C_R, and Sc_t are plotted in Fig. 4 for the two QoIs.

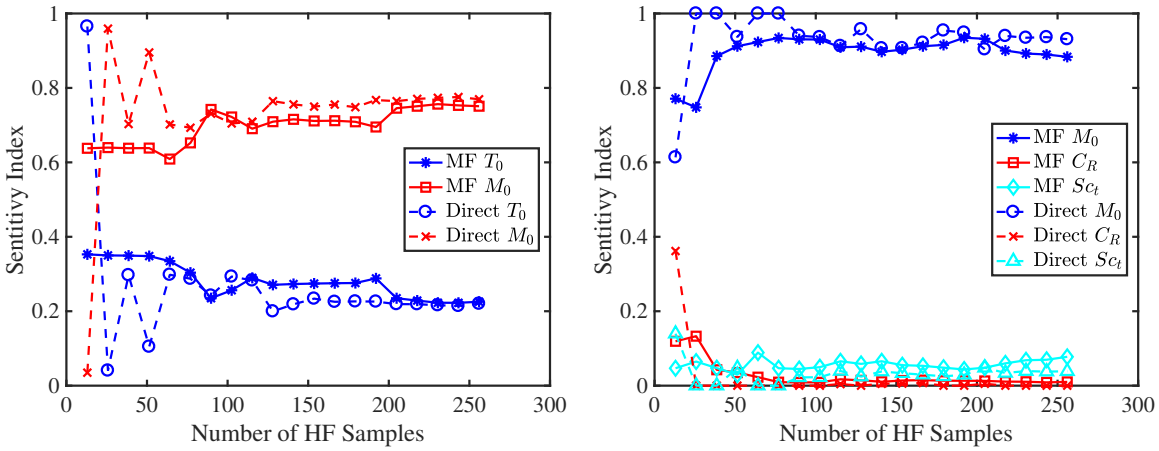

(a) ϕ_B (b) $R_{\bar{P}}$

Figure 4. Sobol indices (total effect sensitivity) for QoIs ϕ_B and $R_{\bar{P}}$, using direct and MF approaches as the number of $d/16$ evaluations varies.

The plots for the direct approach can be very noisy when few samples are available. For instance, the relative importance for T_0 and M_0 are completely switched for ϕ_B at 13 samples. The MF approach produces more stable results in comparison, where the $d/8$ simulations act as a filter. At the left end of zero $d/16$ simulations, the indices coincide with values in Fig. 3(a); at the right end of 256 $d/16$ simulations, the indices are almost equal to those in Fig. 3(b). The minor differences are caused by the summation of PC surrogates in Eqn. (7), where approximation errors in PC do not completely subtract out in the telescopic form. The difference between direct and MF computations diminish as the number of $d/16$ runs increases, but we also observe that the MF approach converges more slowly due to the contamination from the low-fidelity runs. In this particular case, the stabilization benefit from the MF approach appears most useful for fewer than 75 simulations of the $d/16$ model, and the direct approach is preferred outside this regime due to the overhead from extra low-fidelity simulations in the MF approach.

The MF ASQ approach in Sec. III.B is deployed in the reduced four-dimensional parameter space of T_0, M_0, C_R, and Sc_t, constructing the PC surrogate

$$\tilde{f}_2(\lambda(\xi)) = \tilde{f}_1(\lambda(\xi)) + \tilde{f}_{\Delta 2}(\lambda(\xi)) \tag{17}$$

for QoIs ϕ_B and $R_{\bar{P}}$. Refinement tolerances of 2.4×10^{-7} and 3.1×10^{-6} were reached for $\tilde{f}_1$ and $\tilde{f}_{\Delta 2}$, respectively. The construction of $\tilde{f}_1$ required 257 $d/8$ evaluations, and $\tilde{f}_{\Delta 2}$ required 257 $d/8$ and $d/16$ evaluations. Between the two terms, 129 of the $d/8$ runs were at the same quadrature locations, resulting in a total of 385 $d/8$ and 257 $d/16$ actual runs for the entire ASQ procedure (results for overlapping quadrature evaluations were cached and so simulations were not repeated). The final PC surrogate contained basis terms up to degree 11 polynomials, with higher degrees occurring for parameter M_0 for $\tilde{f}_1$, and T_0, M_0, and Sc_t for $\tilde{f}_{\Delta 2}$. The Sobol indices with respect to the four parameters $\{T_0, M_0, C_R, Sc_t\}$ under the overall PC surrogate $\tilde{f}_2$ are $\{0.21, 0.78, 0.10, 0.09\}$ for ϕ_B, and $\{0.16, 0.82, 0.06, 0.15\}$ for $R_{\bar{P}}$. This is qualitatively consistent with observations in Fig. 3(b) from the GSA stage.

Fig. 5 shows marginal probability density functions (PDFs) for the two QoIs, via vertically-normalized histograms (i.e., total histogram area is unity) constructed using 10^5 samples of the PC surrogate. The corresponding kernel density estimate (KDE) of the joint PDF is presented in Fig. 6. These results indicate a multi-modal behavior, possibly corresponding to multiple operating regimes. Correlation between the two QoIs as well as non-Gaussian features are evident in the joint PDF. The mean (μ) and covariance (Σ) estimates for $\{\phi_B, R_{\bar{P}}\}$ are

$$\mu = \begin{bmatrix} 0.2015 \\ 0.3544 \end{bmatrix} \qquad \text{and} \qquad \Sigma = \begin{bmatrix} 1.778 \times 10^{-4} & 1.756 \times 10^{-4} \\ 1.756 \times 10^{-4} & 5.279 \times 10^{-4} \end{bmatrix}. \tag{18}$$

These features will be further investigated in a subsequent paper.

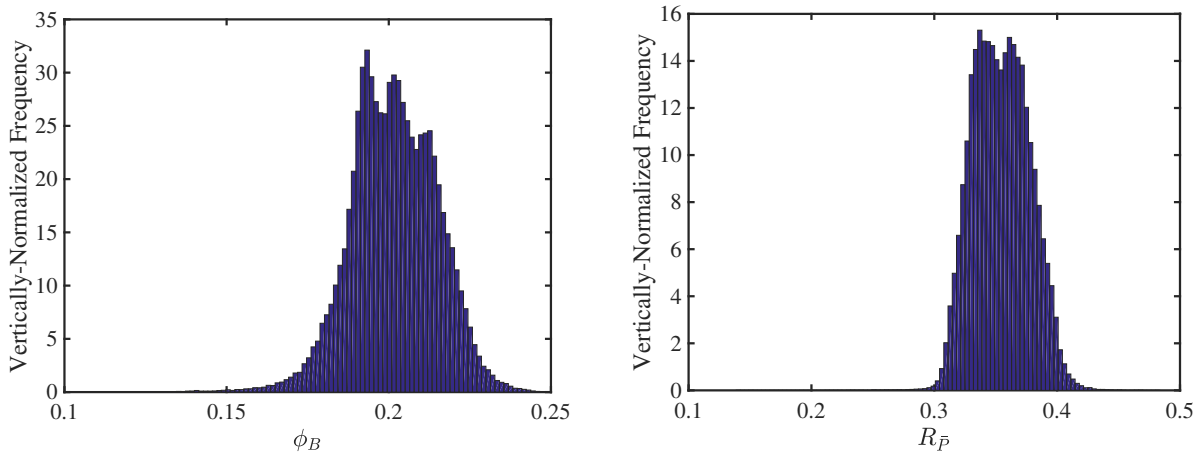

Figure 5. Vertically-normalized histograms for marginal distributions of ϕ_B and $R_{\bar{P}}$, produced using samples generated from PC surrogates.

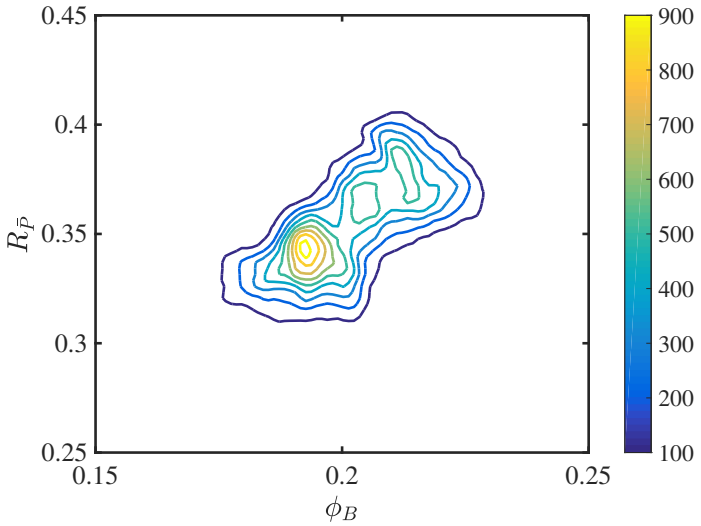

Figure 6. KDE of joint PDF between ϕ_B and $R_{\bar{P}}$, produced using samples generated from the PC surrogate.

V. Conclusions

Uncertainty quantification is an important part of scramjet design, but it is often challenged by expensive flow simulations and high-dimensional parameter spaces. One important tool to help overcome these obstacles is surrogate modeling. Effective surrogates allow a practical computational characterization of statistical properties for quantities of interest under different sources of uncertainty. In this paper, we presented a two-stage, multifidelity (MF) procedure for constructing polynomial chaos (PC) surrogates of performance

metrics from large eddy simulations of supersonic reactive flows inside the HIFiRE Direct Connect Rig combustor.

In the first stage, global sensitivity analysis (GSA) is conducted under a full 11-dimensional parameter space, which reflect uncertainty from inlet and fuel inflow boundary conditions as well as turbulence model parameters. Compressive sensing is employed to discover sparse PC representations based on a small number of randomized simulations. These representations are then used to extract Sobol sensitivity indices. A MF GSA variant was observed to offer numerical stability when very few number of high-fidelity simulations are available, although it required additional low-fidelity runs. Focusing on QoIs reflecting overall scramjet performance (ϕ_B and $R_{\bar{P}}$), the parameters with the highest Sobol sensitivity indices were T_0, M_0, C_R, and Sc_t.

In this reduced parameter space, the second stage involved constructing PC surrogates employing adaptive sparse quadrature. A surrogate was constructed separately for each term in a MF telescopic expansion, while results were cached and reused when repeated quadrature evaluations were requested from the surrogate constructions of different terms. Probability density functions for QoIs and their statistics, including correlation information, were retrieved from the PC surrogates. Overall, MF approaches offer a platform to combine results from multiple models of different fidelity, which can be advantageous by achieving an overall computational efficient path to estimate statistical properties.

Acknowledgments

Support for this research was provided by the Defense Advanced Research Projects Agency (DARPA) program on Enabling Quantification of Uncertainty in Physical Systems (EQUiPS). Sandia National Laboratories is a multimission laboratory managed and operated by National Technology and Engineering Solutions of Sandia, LLC., a wholly owned subsidiary of Honeywell International, Inc., for the U.S. Department of Energy's National Nuclear Security Administration under contract DE-NA-0003525.

References

[1]Witteveen, J., Duraisamy, K., and Iaccarino, G., "Uncertainty Quantification and Error Estimation in Scramjet Simulation," *17th AIAA International Space Planes and Hypersonic Systems and Technologies Conference*, No. 2011-2283, 2011.

[2]Constantine, P. G., Emory, M., Larsson, J., and Iaccarino, G., "Exploiting active subspaces to quantify uncertainty in the numerical simulation of the HyShot II scramjet," *Journal of Computational Physics*, Vol. 302, 2015, pp. 1–20.

[3]Huan, X., Safta, C., Sargsyan, K., Geraci, G., Eldred, M. S., Vane, Z. P., Lacaze, G., Oefelein, J. C., and Najm, H. N., "Global Sensitivity Analysis and Quantification of Model Error for Large Eddy Simulation in Scramjet Design," *19th AIAA Non-Deterministic Approaches Conference*, No. 2017-1089, Grapevine, TX, 2017.

[4]Huan, X., Safta, C., Sargsyan, K., Geraci, G., Eldred, M. S., Vane, Z. P., Lacaze, G., Oefelein, J. C., and Najm, H. N., "Toward Global Sensitivity Analysis and Quantification of Model Error in Scramjet Computations," *Accepted in AIAA Journal*, 2017.

[5]Soize, C., Ghanem, R. G., Safta, C., Huan, X., Vane, Z. P., Oefelein, J. C., Lacaze, G., and Najm, H. N., "Enhancing Model Predictability for a Scramjet Using Probabilistic Learning on Manifolds," *Submitted*, 2018.

[6]Tsilifis, P., Huan, X., Safta, C., Sargsyan, K., Lacaze, G., Oefelein, J. C., Najm, H. N., and Ghanem, R. G., "Compressive sensing adaptation for polynomial chaos expansions," *Submitted*, 2018.

[7]Dolvin, D. J., "Hypersonic International Flight Research and Experimentation (HIFiRE)," *15th AIAA International Space Planes and Hypersonic Systems and Technologies Conference*, No. 2008-2581, Dayton, OH, 2008.

[8]Dolvin, D. J., "Hypersonic International Flight Research and Experimentation," *16th AIAA/DLR/DGLR International Space Planes and Hypersonic Systems and Technologies Conference*, No. 2009-7228, Bremen, Germany, 2009.

[9]Jackson, K. R., Gruber, M. R., and Barhorst, T. F., "The HIFiRE Flight 2 Experiment: An Overview and Status Update," *45th AIAA/ASME/SAE/ASEE Joint Propulsion Conference & Exhibit*, No. 2009-5029, Denver, CO, 2009.

[10]Jackson, K. R., Gruber, M. R., and Buccellato, S., "HIFiRE Flight 2 Overview and Status Uptate 2011," *17th AIAA International Space Planes and Hypersonic Systems and Technologies Conference*, No. 2011-2202, San Francisco, CA, 2011.

[11]Gruber, M. R., Jackson, K., and Liu, J., "Hydrocarbon-Fueled Scramjet Combustor Flowpath Development for Mach 6-8 HIFiRE Flight Experiments," Tech. Rep. AFRL-RZ-WP-TP-2010-2243, AFRL, 2008.

[12]Ferlemann, P. G., "Forebody and Inlet Design for the HIFiRE 2 Flight Test," *JANNAF Airbreathing Propulsion Subcommittee Meeting*, Boston, MA, 2008.

[13]Gruber, M. R., Ferlemann, P. G., and McDaniel, K., "HIFiRE Flight 2 Flowpath Design Update," Tech. Rep. AFRL-RZ-WP-TP-2010-2247, AFRL, 2009.

[14]Hass, N. E., Cabell, K. F., and Storch, A. M., "HIFiRE Direct-Connect Rig (HDCR) Phase I Ground Test Results from the NASA Langley Arc-Heated Scramjet Test Facility," Tech. Rep. LF99-8888, NASA, 2010.

[15]Storch, A. M., Bynum, M., Liu, J., and Gruber, M., "Combustor Operability and Performance Verification for HIFiRE Flight 2," *17th AIAA International Space Planes and Hypersonic Systems and Technologies Conference*, No. 2011-2249, San Francisco, CA, 2011.

[16]Ghanem, R. G. and Spanos, P. D., *Stochastic Finite Elements: A Spectral Approach*, Springer New York, New York, NY, 1st ed., 1991.

[17]Najm, H. N., "Uncertainty Quantification and Polynomial Chaos Techniques in Computational Fluid Dynamics," *Annual Review of Fluid Mechanics*, Vol. 41, 2009, pp. 35–52.

[18]Xiu, D., "Fast Numerical Methods for Stochastic Computations: A Review," *Communications in Computational Physics*, Vol. 5, No. 2-4, 2009, pp. 242–272.

[19]Le Maître, O. P. and Knio, O. M., *Spectral Methods for Uncertainty Quantification: with Applications to Computational Fluid Dynamics*, Springer Netherlands, Houten, Netherlands, 2010.

[20]Ng, L. W. T. and Eldred, M., "Multifidelity Uncertainty Quantification Using Non-Intrusive Polynomial Chaos and Stochastic Collocation," *53rd AIAA/ASME/ASCE/AHS/ASC Structures, Structural Dynamics and Materials Conference*, No. 2012-1852, Honolulu, Hawaii, 2012.

[21]Eldred, M. S., Ng, L. W. T., Barone, M. F., and Domino, S. P., "Multifidelity Uncertainty Quantification Using Spectral Stochastic Discrepancy Models," *Handbook of Uncertainty Quantification*, Springer International Publishing, Cham, 2015, pp. 1–45.

[22]Peherstorfer, B., Willcox, K., and Gunzburger, M., "Survey of multifidelity methods in uncertainty propagation, inference, and optimization," Tech. Rep. ACDL Technical Report TR16-1, Massachusetts Institute of Technology, 2016.

[23]Geraci, G., Eldred, M. S., and Iaccarino, G., "A multifidelity multilevel Monte Carlo method for uncertainty propagation in aerospace applications," *19th AIAA Non-Deterministic Approaches Conference*, No. 2017-1951, Grapevine, TX, 2017.

[24]Gerstner, T. and Griebel, M., "Numerical integration using sparse grids," *Numerical Algorithms*, Vol. 18, 1998, pp. 209–232.

[25]Barthelmann, V., Novak, E., and Ritter, K., "High dimensional polynomial interpolation on sparse grids," *Advances in Computational Mathematics*, Vol. 12, 2000, pp. 273–288.

[26]Gerstner, T. and Griebel, M., "Dimension-Adaptive Tensor-Product Quadrature," *Computing*, Vol. 71, No. 1, 2003, pp. 65–87.

[27]Saltelli, A., Tarantola, S., Campolongo, F., and Ratto, M., *Sensitivity Analysis in Practice: A Guide to Assessing Scientific Models*, John Wiley & Sons, Chichester, United Kingdom, 2004.

[28]Saltelli, A., Ratto, M., Andres, T., Campolongo, F., Cariboni, J., Gatelli, D., Saisana, M., and Tarantola, S., *Global Sensitivity Analysis: The Primer*, John Wiley & Sons, Chichester, United Kingdom, 2008.

[29]Candès, E. J., Romberg, J., and Tao, T., "Robust Uncertainty Principles: Exact Signal Reconstruction From Highly Incomplete Frequency Information," *IEEE Transactions on Information Theory*, Vol. 52, No. 2, 2006, pp. 489–509.

[30]Donoho, D. L., "Compressed sensing," *IEEE Transactions on Information Theory*, Vol. 52, No. 4, 2006, pp. 1289–1306.

[31]Pellett, G. L., Vaden, S. N., and Wilson, L. G., "Opposed Jet Burner Extinction Limits: Simple Mixed Hydrocarbon Scramjet Fuels vs Air," *43rd AIAA/ASME/SAE/ASEE Joint Propulsion Conference & Exhibit*, No. 2007-5664, Cincinnati, OH, 2007.

[32]Lu, T. and Law, C. K., "A directed relation graph method for mechanism reduction," *Proceedings of the Combustion Institute*, Vol. 30, No. 1, 2005, pp. 1333–1341.

[33]Zambon, A. C. and Chelliah, H. K., "Explicit reduced reaction models for ignition, flame propagation, and extinction of C2H4/CH4/H2 and air systems," *Combustion and Flame*, Vol. 150, No. 1-2, 2007, pp. 71–91.

[34]Smith, G. P., Molden, D. M., Frenklach, M., Moriarty, N. W., Eiteneer, B., Goldenberg, M., Bowman, C. T., Hanson, R. K., Song, S., Gardiner, W. C. J., Lissianski, V. V., and Qin, Z., "GRI-MECH 3.0," http://www.me.berkeley.edu/gri_mech/, (accessed 2017-12-12).

[35]Lacaze, G., Vane, Z. P., and Oefelein, J. C., "Large Eddy Simulation of the HIFiRE Direct Connect Rig Scramjet Combustor," *55th AIAA Aerospace Sciences Meeting*, No. 2017-0142, Grapevine, TX, 2017.

[36]Oefelein, J. C., "Large eddy simulation of turbulent combustion processes in propulsion and power systems," *Progress in Aerospace Sciences*, Vol. 42, No. 1, 2006, pp. 2–37.

[37]Oefelein, J. C., *Simulation and Analysis of Turbulent Multiphase Combustion Processes at High Pressures*, Ph.D. thesis, The Pennsylvania State University, 1997.

[38]Oefelein, J. C., Schefer, R. W., and Barlow, R. S., "Toward Validation of Large Eddy Simulation for Turbulent Combustion," *AIAA Journal*, Vol. 44, No. 3, 2006, pp. 418–433.

[39]Oefelein, J. C., Lacaze, G., Dahms, R., Ruiz, A., and Misdariis, A., "Effects of Real-Fluid Thermodynamics on High-Pressure Fuel Injection Processes," *SAE International Journal of Engines*, Vol. 7, No. 3, 2014, pp. 1125–1136.

[40]Lacaze, G., Misdariis, A., Ruiz, A., and Oefelein, J. C., "Analysis of high-pressure Diesel fuel injection processes using LES with real-fluid thermodynamics and transport," *Proceedings of the Combustion Institute*, Vol. 35, No. 2, 2015, pp. 1603–1611.

[41]Xiu, D. and Karniadakis, G. E., "The Wiener-Askey Polynomial Chaos for Stochastic Differential Equations," *SIAM Journal on Scientific Computing*, Vol. 24, No. 2, 2002, pp. 619–644.

[42]Sobol, I. M., "Theorems and examples on high dimensional model representation," *Reliability Engineering & System Safety*, Vol. 79, No. 2, 2003, pp. 187–193.

[43]Boyd, S., Parikh, N., Chu, E., Peleato, B., and Eckstein, J., "Distributed Optimization and Statistical Learning via the Alternating Direction Method of Multipliers," *Foundations and Trends in Machine Learning*, Vol. 3, No. 1, 2010, pp. 1–122.

[44]Boyd, S., Parikh, N., Chu, E., Peleato, B., and Eckstein, J., "Solve LASSO via ADMM," https://web.stanford.edu/~boyd/papers/admm/lasso/lasso.html, 2011, (accessed 2017-07-02).

[45]Huan, X., Safta, C., Sargsyan, K., Vane, Z. P., Lacaze, G., Oefelein, J. C., and Najm, H. N., "Compressive Sensing with Cross-Validation and Stop-Sampling for Sparse Polynomial Chaos Expansions," *arXiv preprint arXiv:1707.09334*, 2017.